Dynamics of oxygen ordering in the cell-doubled phase of $YBa_2Cu_3O_{6+x}$

P. J. Kundrotas,* E. E. Tornau,† and A. Rosengren
Department of Theoretical Physics, The Royal Institute of Technology, S–100 44 Stockholm, Sweden
(Received 25 March 1996)

The dynamics of domain growth, related to oxygen ordering into the cell-doubled orthorhombic phase of $YBa_2Cu_3O_{6+x}$, was studied. The growth, described using Monte Carlo simulations of the asymmetric next-nearest-neighbor interaction model without impurities, after annealing and quench from finite temperatures is found to be different at early and late times. At early times of domain growth a growth exponent $n \approx 0.25$ is observed for both nearest-neighbor (NN) and next-nearest-neighbor diffusion and $n \approx 0.15$ for NN diffusion only. At late times the growth behavior is very close to $\log t$ which is related to the anisotropy of the O-Cu-O chains. The growth dynamics in the case of a small amount of cation substitutional impurities supports the idea that the logarithmic behavior is an intrinsic property of the model chosen and depends very little on impurities. [S0163-1829(96)07330-4]

I. INTRODUCTION

The time evolution of a system ordering towards equilibrium is an interesting problem of statistical as well as condensed matter physics. The dynamics of domain growth for the Ising model, for instance, was thoroughly investigated by many authors (see, e.g., Refs. 1–4). These studies were mostly restricted to the isotropic systems. The extension to anisotropic systems is highly motivated for the following reason: there are compounds which exhibit ordering governed by a strong anisotropy. Oxygen ordering in the high temperature superconductor $YBa_2Cu_3O_{6+x}$ is a typical example of such a process.

The structure of this compound depends on the concentration x and order of the oxygen atoms in the basal plane. The main orthorhombic structure of this compound, the so-called O_I phase with stoichiometry $x=1$, exhibits long-range order (sharp Bragg peaks). Contrary to what is found for this phase, sharp Bragg peaks do not emerge at the superstructure positions of the other orthorhombic low-temperature phases.[5–7] The O_{II} phase with stoichiometry $x=0.5$ and the O_{III} phase with stoichiometry $x=0.67$ demonstrate short-range order and quasi-two-dimensional character of their ordering into O-Cu-O chains along the b axis. The correlation lengths along the main axes (given in units of lattice cells), obtained by neutron and x-ray diffraction studies, are $\xi_a=10.2$, $\xi_b=44.5$ ($x=0.5$) (Ref. 6) and $\xi_a=5$ and $\xi_b=19$ ($x=0.77$) (Ref. 7) for the O_{II} and the O_{III} superstructures, respectively.

It was demonstrated in an early Monte Carlo (MC) study[8] of the oxygen ordering dynamics of $YBa_2Cu_3O_{6+x}$ that the excess energy decreases with time according to a power law. However, in a recent x-ray diffraction study by Schleger *et al.*,[6] it was found for the $x=0.5$ sample that the domain growth only in the beginning follows the Allen-Cahn power-law behavior. At later times the domain growth was found to be logarithmic in time below the phase transition to the O_{II} phase. The idea was therefore raised that random field effects (RFE) are responsible for the short-range order of the O_{II} phase. As possible causes for the RFE, Cu(1) chain-site substitutional impurities, strain fields arising from twin domain boundaries, dislocations, or even a rearrangement of the oxygen atoms were mentioned.

In this paper we study numerically whether an oxygen rearrangement in the pure or slightly cation substituted O_{II} phase can be considered as the cause of RFE. We want to answer the question if the RFE are an intrinsic property of such a complex anisotropic model, which is used to describe the oxygen ordering in $YBa_2Cu_3O_{6+x}$, or if the RFE are caused by the impurities. The dynamics of domain growth is studied for a system which is quenched from temperatures corresponding to the tetragonal phase of the compound down to temperatures below the transition point to the O_{II} phase. The modelling of oxygen ordering in $YBa_2Cu_3O_{6+x}$ is usually performed using the asymmetric next-nearest-neighbor interaction (ASYNNNI) model[9] which exhibits a rich phase (T,x) diagram.[10] With the inclusion of an extra longer-range term this model demonstrates a variety of phase transitions, comprising first-order transitions[11] and even transitions to incommensurate phases.[12]

II. THE MODEL

The ASYNNNI lattice-gas model has the Hamiltonian

$$\mathcal{H}_0 = v_1 \sum_{\mathrm{NN}} n_i^k n_j^l + v_2 \sum_{\substack{\mathrm{NNN} \\ (\mathrm{over\ Cu})}} n_i^k n_j^k + v_3 \sum_{\mathrm{NNN}} n_i^k n_j^l - (\mu+\epsilon)\sum_i n_i^k , \tag{1}$$

where $n_i=0, 1$ is the occupancy number of the oxygen site i in the basal CuO_x plane of 123. Here the sums run over the sets of nearest (NN) and next-nearest (NNN) neighbor oxygen sites of the k, $l=O(1)_1$, $O(1)_2$, and O(5) sublattices, μ is the chemical potential, and ϵ is the site binding energy. We use the crystallographic notation for the oxygen atoms, taking also into account that, in the O_{II} phase, the O(1) sublattice splits into two sublattices. Note, that if we have to consider chains running along the a axis as well, as in the case of Cu substitutions (see the Sec. III b), the O(5) sublattice too splits into two sublattices, $O(5)_1$ and $O(5)_2$. The

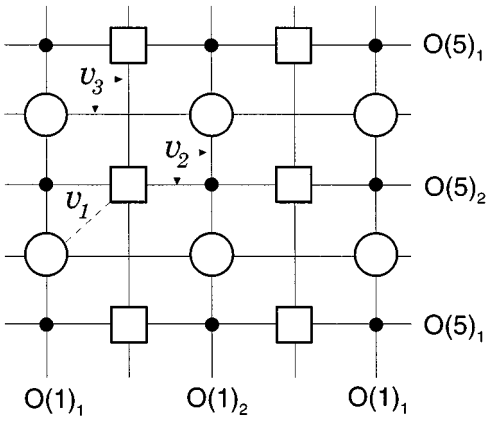

FIG. 1. The basal plane of $YBa_2Cu_3O_{6+x}$ with different sublattices and constants of interaction demonstrated. Oxygen sites of the $O(1)_1$ and $O(1)_2$ sublattices are shown by the open circles, oxygen sites of the $O(5)_1$ and $O(5)_2$ sublattices by open squares, and copper atoms by small filled circles.

sublattices and the interaction constants of the oxygen atoms are shown in Fig. 1. The ground state of the O_I phase corresponds to fully occupied $O(1)_1$ and $O(1)_2$ sublattices and a vacant $O(5)=O(5)_1+O(5)_2$ sublattice, $c_{O(1)_1}=c_{O(1)_2}=1$, $c_{O(5)}=0$. Here $c_k=\langle n_i^k\rangle$ are the sublattice oxygen concentrations. The ground state of the O_{II} phase ($x=0.5$) corresponds to $c_{O(1)_1}=1$ and $c_{O(1)_2}=c_{O(5)}=0$. The total oxygen content of the CuO_x plane is $x=(c_{O(1)_1}+c_{O(1)_2}+2c_{O(5)})/2$.

The ASYNNNI model (1) with attractive v_2 and repulsive v_1 and v_3 interactions, gives a (T,x) phase diagram containing the experimentally observed structures [tetragonal, O_I and O_{II} (Ref. 10)]. In the present study we use the values of the interaction constants obtained by Sterne and Wille[13] from first-principles calculation: $v_1=4358$ K, $v_2/v_1=-0.35$ and $v_3/v_1=0.16$. For this set of interaction constants the maximum of the O_{II} phase in the phase diagram is at $T/v_1=0.126$ and $x=0.5$, and the room temperature section is correspondingly at $T/v_1=0.07$.

We study here the dynamics of oxygen ordering in the ASYNNNI model for oxygen concentrations corresponding to the O_{II} phase ($x=0.5$). Similar calculations were performed in Ref. 8, where the system quenched from infinite temperatures to temperatures well inside the O_{II} phase was studied. These simulations were carried out assuming that oxygen atoms diffuse via hopping over NN and NNN sites. In that study the initial growth of domains was explored, i.e., the process while the O(5) sublattice still is occupied. The exponent describing the growth of the linear size of a domain was found to be $n=0.25$-0.35 for the O_{II} phase.

In view of the basal plane interactions, oxygen diffusion by means of NN hopping only is the most probable. The simulations in this case are time consuming and sometimes the system gets ''locked-in'' in a metastable state with very slow kinetics of the domain walls. In this paper we study this type of oxygen diffusion as well and compare it to that which allows also for hopping of the NNN oxygen atoms. In order to describe the experimental data,[6] we anneal the samples at finite temperatures somewhat above the tetragonal to the

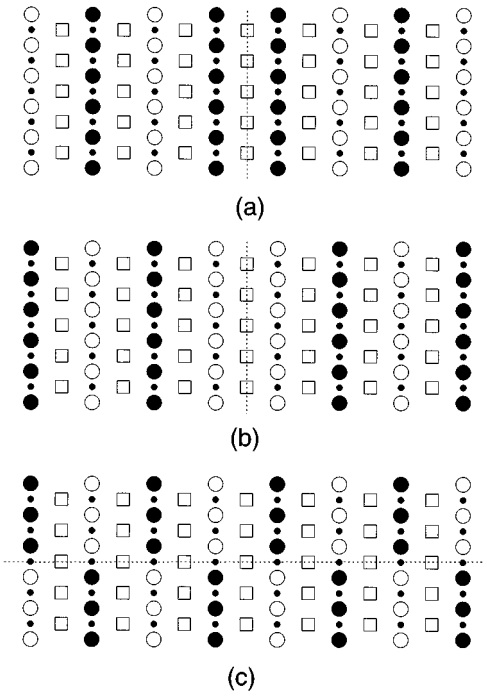

FIG. 2. Three types of interfaces in a late stage of domain growth. The symbols are the same as for Fig. 1. Additionally, large filled circles represent occupied sites of the $O(1)_1$ and $O(1)_2$ sublattices.

O_{II} phase transition ($T/v_1=0.15$) and then perform quenches into the O_{II} phase down to $T/v_1=0.1$, 0.07, and 0.05.

Our simulations were performed using Kawasaki dynamics for a square lattice of the size 64×64. To make sure that our results are not caused by finite-size effects, some simulations were also performed for the 128×128 lattice. The annealing time for the system with randomly chosen initial oxygen arrangement was 5000 MCS/site.

For the case of NN hopping only we conclude the simulation after 5×10^5 MCS/site. For the case of both NN and NNN hopping the time required for the system to reach equilibrium is about one order of magnitude shorter. In both cases the ordering due to the disappearance of the oxygen atoms in the O(5) sublattice is found to be fast, and this sublattice becomes almost empty during the time of annealing. The occurring domains are related to ordering in the sublattices $O(1)_1$ and $O(1)_2$. Snapshots of possible types of domain walls are shown in Fig. 2. These walls are caused by a two-fold degeneracy of the O_{II} phase when the O(5) sublattice becomes empty (the system is fourfold degenerate before). The domain wall is caused either by two neighboring occupied (or empty) O-Cu-O chains belonging to different O(1) sublattices [see Fig. 2(a) and 2(b)] or by the interface shown in Fig. 2(c).

To reduce the effect of fluctuations, which might occur within a single MC run, the calculated parameters were averaged over different runs. For each quench temperature 20 runs were performed. Three typical sets of the time dependence of the $O(1)_1$ and $O(1)_2$ sublattices oxygen concentrations are shown in Fig. 3. For calculations restricted to NN hopping only the number of (a)-type runs varied from 9 to

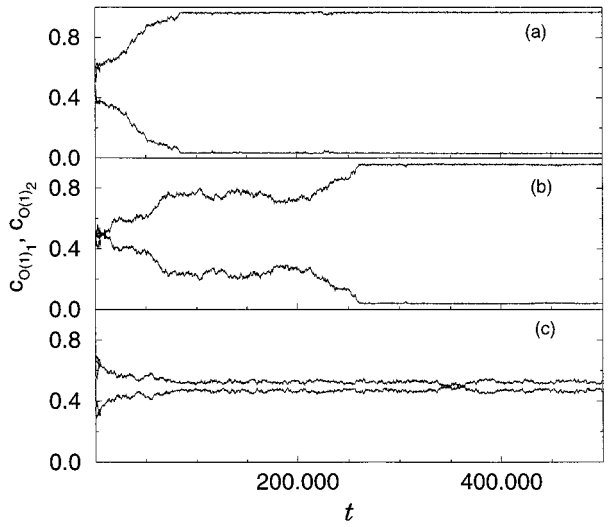

FIG. 3. Three typical time dependences of the order parameter of the O_{II} phase: (a) successful, (b) intermediate, and (c) locked in. Time is given in MCS/site.

12. The numbers of ''successful'' (a)-type and ''unsuccessful'' (c)-type runs were almost equal depending, though weakly, on quench temperatures. About 2–3 runs were of the intermediate (b) type when domain evolution is suspended for a time interval of $1–2\times10^5$ MCS/site. Almost all of our runs for the case of both NN and NNN hopping were ''successful.'' This analysis is important to determine the behavior of domain growth (see discussion in Sec. III A).

A main characteristic of domain evolution with time t is the excess energy of the system $\Delta E(t)=E(t)-E(\infty)$, where $E(\infty)$ is the equilibrium energy. Another important parameter is the average length of the O-Cu-O chains, $\langle l\rangle$, which is a measure of the linear size of a domain.[1,8] For exponential domain growth the following relation is valid

$$\langle l\rangle\sim(\Delta E)^{-1}\sim t^n, \tag{2}$$

where the growth exponent n depends on the nature of the domain walls. For studies of domain growth in the ASYNNNI model also the order parameter of the O_{II} phase $\eta=c_{O(1)_1}-c_{O(1)_2}$ is introduced. If multiplied by the linear size of the MC lattice, it gives an effective linear size of the domains characteristic to the O_{II} phase. An analogous parameter was first introduced for a lattice-gas model with repulsive NN and NNN interactions by Sadiq and Binder.[2] It was shown in that paper that relation (2) with $\langle l\rangle$ substituted by such an effective domain size holds quite well for Glauber dynamics, but is not always satisfied for Kawasaki dynamics. The parameter η, however, has a meaning only (1) for the case of the ''successful'' runs described in Fig. 3(a), and (2) when the O(5) sublattice is already empty.

The condition (1) is almost always satisfied for NN and NNN hopping and for approximately half of the runs for NN hopping only. Thus, the results for $\eta(t)$ growth for the latter type of diffusion should be obtained by averaging over ''successful'' runs only. The consequences of an inclusion of ''locked-in'' runs in the average are discussed below. At late stages of domain growth condition (2) is always satisfied in our calculations.

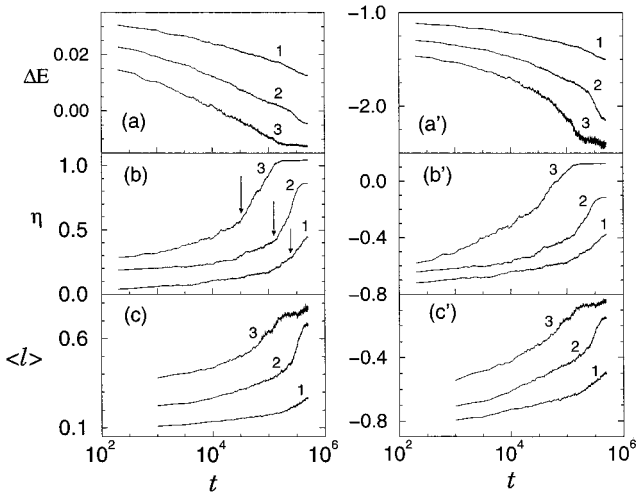

FIG. 4. Semilog and log-log plots of the time dependence of the excess energy (a and a′), the order parameter of the O_{II} phase η (b and b′), and the average length $\langle l\rangle$ of the O-Cu-O chain (c and c′) obtained for NN hopping only. The curves correspond to quench temperatures $T/v_1=0.05$ (1), 0.07 (2), and 0.1 (3). For clarity the curves are shifted with respect to each other along the vertical axis. The arrows mark the crossover time from power-law to logarithmic behavior, t_{cr}.

III. RESULTS AND DISCUSSIONS

A. No impurities

The results of our simulations for NN hopping only are presented in Fig. 4. The results for NN as well as NNN hopping are shown in Fig. 5.

The process of domain growth is found to be quite different at early and late times. At early times of domain dynamics the growth exponent $n\approx0.25$ is observed for both NN and NNN hopping (time interval up to $t_{cr}\approx1000$ MCS/site) and $n\approx0.15$ for NN hopping only (up to $t_{cr}\approx30000$ MCS/site) for the quenches to $T/v_1=0.1$ and 0.07. For quenches to 0.05, n is approximately 0.22 and 0.10, respectively. These results are obtained for ΔE and η. The exponents for $\langle l\rangle$ are 10% lower. Here t_{cr} defines the crossover point above which domain growth starts to demonstrate a behavior very close to

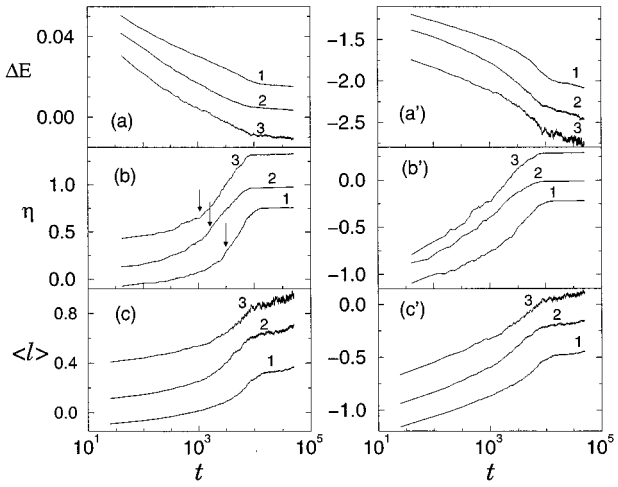

FIG. 5. Same as in Fig. 4, but for NN and NNN hopping.

logarithmic. Straight lines for $t > t_{cr}$ are best seen in the semi-log plots of Figs. 4(b) and 5(b). They are not so pronounced in the time dependence of the excess energy and $\langle l \rangle$. The t_{cr} point might be determined also from a $\log R - \log t$ plot, where $R = \langle l \rangle, \eta$ or $(\Delta E)^{-1}$, as the intersection of the straight line with a slope n at earlier times with the curve at later time which has its slope decreasing with time characteristic to a logarithmic behavior. As might be anticipated, the lower the quench temperature the later the system reaches the logarithmic behavior.

The transition to the late-time regime is related to the fact that the O(5) sublattice becomes empty and all interfaces occurring due to the existence of O-Cu-O chains along different directions vanish. The system turns out to be highly anisotropic in the sense that only the chains along the b axis are left. Thus, only the three types of interfaces shown in Fig. 2 are observed for $t > t_{cr}$.

The domain growth for $t > t_{cr}$ is related to the gradual disappearance of the interfaces of Fig. 2. The time dependence of the characteristic parameters of domain growth and the t_{cr} dependence on quench temperature are qualitatively very similar to the time dependence of the correlation length obtained in the x-ray diffraction study of $YBa_2Cu_3O_{6.5}$ (Ref. 6): an early-time power-law growth with a transition to a late-time logarithmic behavior. However, for the power-law regime we find much lower values of n, especially for NN hopping only, than what Allen-Cahn growth gives $(n = 1/2)$.[6]

An obvious difference between our results obtained for NN and NNN and NN hopping only is the time scale, which clearly shifts due to the slower NN hopping only. This fact is reflected, e.g., in the time t_{cr} at which the logarithmic behavior of growth parameters starts. Note, however, that the time interval of logarithmic behavior in a logarithmic scale is almost the same $\Delta \log(t) \sim 0.8$ for both types of diffusion, though the real time scale is very different.

Another important difference between the two types of hopping is observed by comparing the excess energy (or the parameter $\langle l \rangle$) for NN hopping only obtained by averaging over all possible runs and by averaging only over successful runs (see Fig. 6). There is no difference at early stages. It turns out, however, that the late stage logarithmic behavior is less and less evident if more and more locked-in [Fig. 3(b) and 3(c)] runs are included in the average. This fact allows us to make an important distinction between the results for NN and NNN hopping (successful runs) and only NN hopping (partly successful runs). If NN hopping only best describes the dynamics of oxygen ordering in the basal plane of $YBa_2Cu_3O_{6+x}$, then the late-stage logarithmic behavior might be questionable. Of course, it might be argued that all runs are successful in the sense that sooner or later the parameter η would start to grow if one just waits long enough. But the average would anyhow not show logarithmic behavior. On the other hand, if there would be some supporting evidence for both NN and NNN diffusion in $YBa_2Cu_3O_{6+x}$ (if, e.g., the oxygen vacancies in the neighboring BaO planes would mediate such a type of diffusion) then our results would clearly point to a late stage logarithmic behavior of domain growth.

Taking the anisotropy in the late stages of domain growth and the differences of the two types of diffusion into account, we can only speculate why the logarithmic behavior was not seen for the quenches from infinite temperature.[8] According to Poulsen *et al.*,[8] in the latter case the oxygen atoms in the O(5) sublattice remain in their positions for very long times, creating therefore extra interfaces (not shown in Fig. 2) due to the existence of chains perpendicular to each other. We have also performed simulations for NN and NNN hopping for quenches from infinite temperatures. We find that the O(5) sublattice is occupied considerably longer than in the case of finite-temperature annealing. However, after the depletion of this sublattice ($t \sim t_{cr}$) both systems behave identically (Fig. 7), both demonstrating a logarithmic behavior. As might be seen from Fig. 7, the growth behavior is different for the two cases in the early stage ($t < t_{cr}$): for quenches from infinite temperatures a growth exponent $n \approx 0.25$ for very early times is followed by $n \approx 0.35$–0.4 in accordance with Ref. 8, while for quenches from finite temperature the exponent $n \approx 0.25$ holds all the way up to

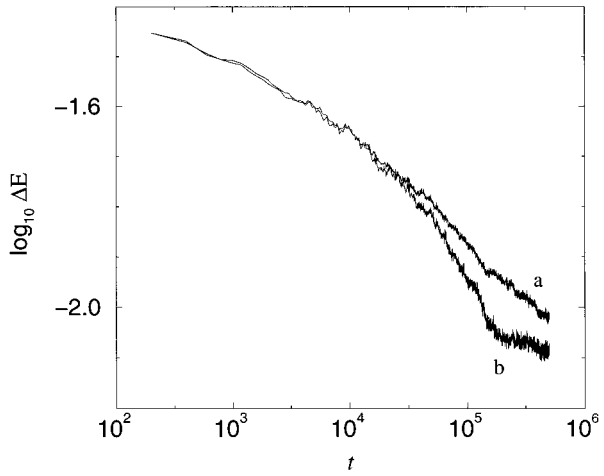

FIG. 6. Difference in time dependence of excess energy for NN hopping obtained by averaging over all possible runs (a) and by averaging only over successful [Fig. 3(a)] runs (b). Quench temperature $T/v_1 = 0.1$.

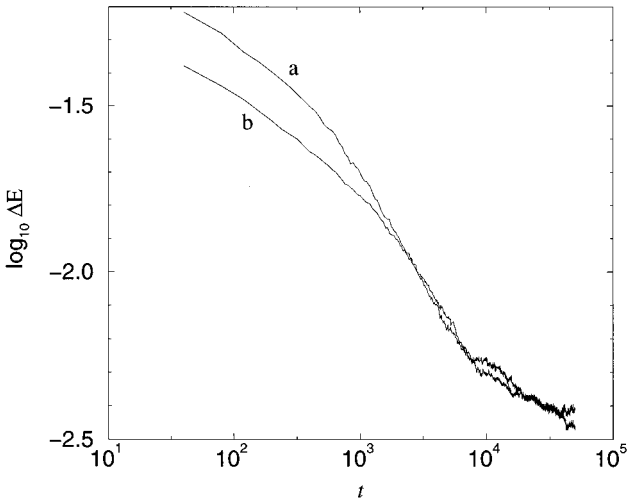

FIG. 7. The difference in excess energy for quenches to $T/v_1 = 0.07$ from ''infinite'' (a) and finite, $T/v_1 = 0.15$, (b) temperatures. The simulation is performed using NN and NNN diffusion.

$t=t_{cr}$. The change from $n\approx 0.25$ to $n\approx 0.35$–0.4 might be understood from how the O(5) sublattice disappears. This sublattice splits into two sublattices $O(5)_1$ and $O(5)_2$, and the disappearance of the $O(5)_2$ after $t\approx 1000$ MCS/site correlates with the change of n, while the following disappearance of the $O(5)_1$ after $t\approx 2000$ MCS/site—with t_{cr} (here the numbers are approximate and given for NN and NNN diffusion). For a quench from finite-temperature both O(5) sublattices disappear very fast. Thus, the most probable reason why the logarithmic behavior of the growth parameters was not noticed for the quenches from infinite temperature,[8] is that the system in that case was not ''sufficiently'' anisotropic: the O(5) sublattice was not empty and the ''locked-in'' runs, shown in Fig. 3(c), dominated the average. It should be noted, that this was not the case for our simulations of domain growth for NN and NNN hopping.

Comparing the time dependences of the two parameters characterizing domain size, $\langle l\rangle$ and η, some differences are found. At late times, when the occupancy of the O(5) sublattice is zero, the order parameter η saturates to almost 1, while the saturation value of the average chain length is limited to 0.6–0.7 of the linear size of the lattice. The reason why there is an incomplete saturation of the order parameters is found from an analysis of the snapshots. It happens at late stages of chain growth that a short chain in sublattice $O(1)_2$ will be locked between two ''infinite'' chains (i.e., the ends of these chains are connected by the periodic boundary conditions) in sublattice $O(1)_1$. Due to the interactions imposed in our model, the oxygen atoms of such a short chain might move only along the channel created by the two ''infinite'' chains, break up ''their'' chain and then stick again together. The probability for an ''infinite'' chain to break up (and allow for a short chain to dilute out) is in this case very low. This locking might change the value of $\langle l\rangle$ considerably, though the saturation threshold for the parameter η is still around 0.95. Thus, for later times η is a better characteristic of the average linear size of the O_{II} phase domain, since $\langle l\rangle$ describes the length along the preferential b axis, neglecting the length of the domain in the perpendicular direction, while η effectively describes the average size of the growing O_{II} phase domain. However, for early times, when the O(5) sublattice is still occupied, the average length of a chain $\langle l\rangle$ takes the chains existing in all sublattices into account. The parameter η describes only changes in the sublattices $O(1)_1$ and $O(1)_2$. Thus, for a description of the *overall* growth dynamics at early stages, especially for systems quenched from very high temperatures, the parameter $\langle l\rangle$ [or equivalently $(\Delta E)^{-1}$] is more appropriate than η.

B. The effect of impurities

Here we study the possibility that RFE might occur due to the substitution of Cu in the basal plane by a cation with a higher oxygen coordination. We rely on an experimental observation that in $YBa_2Cu_3O_{6+x}$ (especially that grown in Al crucibles) impurities are present at the basal plane copper positions. The concentration of these impurities even in a high-purity single crystal can be around 0.1%.[6] For our calculations we choose small amounts of Al impurities.

The attractive interaction between Al and O ions is stronger than that between Cu and O, therefore, contrary to being four-coordinated as Cu^{2+}, Al^{3+} prefers a sixfold oxygen coordination. This fact can be considered in our model in a way described in Ref. 14: the site binding energy of an oxygen atom, ε, depends on its attractive interaction with the two closest metal atoms. To get a higher coordination of Al than that of Cu, it is reasonable to assume that the site binding energy of oxygen next to Al, ε_{Al}, is much larger than ε_{Cu}, and that $\varepsilon_{Al}\gg|v_1|$. We take $\varepsilon_{Al}/|v_1|=5$.

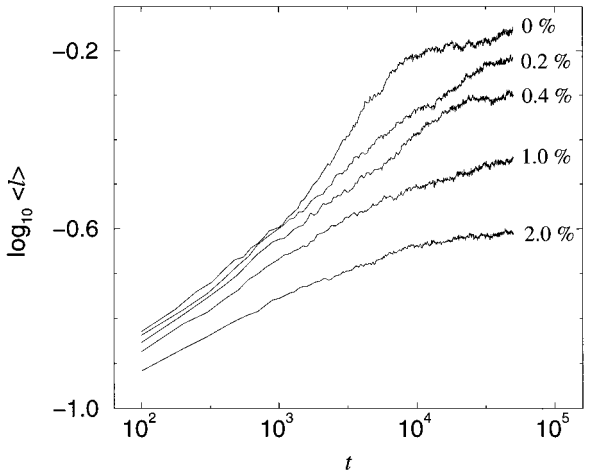

FIG. 8. Log-log plot of the time dependence of the average length obtained for the model with impurities for NN and NNN diffusion and quench temperature $T/v_1=0.07$. For clarity the curves are shifted with respect to each other along the vertical axis.

After what was found for the pure ASYNNNI model, we anticipated that the effect of impurities in a small amount (which means that the O_{II} phase is not yet destroyed) might cause the disappearance of the late-time logarithmic behavior of the growth parameters. There were two reasons for that. First, the introduction of impurities leads to the formation of chains, directed along both the a and b axes and intersecting each other at an impurity site.[15] Second, with an increasing amount of impurities, we expected that most of our runs would be of Fig. 3(c) type which blur the logarithmic behavior. Both factors would destroy the anisotropy needed for the occurrence of the RFE in the ASYNNNI model.

That this is really the case is seen from Fig. 8, where the time dependence of the average length of the domain for NN and NNN diffusion is presented for the Al impurity concentration, c_{Al}, up to 2%. The cusp at $c_{Al}=0$, which is the manifestation of the logarithmic behavior, disappears for small values of c_{Al} (0.2, 0.4%). However, for $c_{Al}\geqslant 0.5\%$ it is seen that the curves start to bend again at late time implying a new type of behavior. It thus looks like a very small amount of impurities destroys the RFE, which are due to the anisotropy of the model. Impurities in larger amount, though, are likely creating RFE of their own. However, we could not verify this assumption, since for $c_{Al}\geqslant 2\%$ domain growth dynamics starts to be very complicated.

CONCLUSIONS

In summary, simulations of oxygen ordering dynamics for two types of diffusion (NN hopping only and both NN and NNN hopping) were performed for the O_{II} phase of

$YBa_2Cu_3O_{6+x}$ using the ASYNNNI model. It is found that the domain growth dynamics of this system is different at early and late stages. At early stages the domain growth could be described by growth exponents which are found to be different for the two types of oxygen diffusion. At later stages a transition to a logarithmic behavior of the parameters characterizing the domain growth is observed which is caused by the anisotropy of the O-Cu-O chains. This might be the reason of the random field effects observed experimentally for $YBa_2Cu_3O_{6.5}$. The effect of impurities with higher oxygen coordination than copper is shown to be different than in other systems: instead of creating random fields, a small amount of impurities destroys the anisotropy, the main cause of the random field effects in this system. It is further found likely that higher concentrations of such impurities cause random fields of a different nature.

ACKNOWLEDGMENTS

This work was supported by The Swedish Natural Science Council and partly by Grant No. LHT 100 from The International Science Foundation. P.K. is indebted to the Knut and Alice Wallenberg Foundation.

*Also at Faculty of Physics, Vilnius University, Saulėtekio 9, 2054 Vilnius, Lithuania.

†Also at Semiconductor Physics Institute, Goštauto 11, 2600 Vilnius, Lithuania.

[1] G. S. Grest and D. J. Srolovitz, Phys. Rev. B **32**, 3014 (1985).

[2] A. Sadiq and K. Binder, J. Stat. Phys. **35**, 517 (1984).

[3] D. A. Huse, Phys. Rev. B **34**, 7845 (1986).

[4] C. Roland and M. Grest, Phys. Rev. B **39**, 11 971 (1989).

[5] T. Zeiske, D. Hohlwein, R. Sonntag, F. Kubanek, and T. Wolf, Physica C **194**, 1 (1992); D. Hohlwein, in *Materials and Crystallographic Aspects of High-T_c Superconductivity*, edited by E. Kaldis (Kluwer Press, Dortrecht, 1994).

[6] P. Schleger, R. Hadfield, H. Casalta, N. H. Andersen, H. F. Poulsen, M. von Zimmermann, J. R. Schneider, Ruixing Liang, P. Dosanjh, and W. N. Hardy, Phys. Rev. Lett. **74**, 1446 (1995).

[7] P. Schleger, H. Casalta, R. Hadfield, H. F. Poulsen, M. von Zimmermann, N. H. Andersen, J. R. Schneider, Ruixing Liang, P. Dosanjh, and W. N. Hardy, Physica C **241**, 103 (1995).

[8] H. Poulsen, N. H. Andersen, J. V. Andersen, H. Bohr, and O. G. Mouritsen, Phys. Rev. Lett. **66**, 465 (1991); H. V. Poulsen, Ph. D. thesis, Risø National Laboratory, Denmark, 1991.

[9] L. T. Wille, A. Berrera, and D. de Fontaine, Phys. Rev. Lett. **60**, 1065 (1988).

[10] V. E. Zubkus, S. Lapinskas, and E. E. Tornau, Physica C **159**, 501 (1989); **166**, 472 (1990).

[11] G. Grigelionis, S. Lapinskas, A. Rosengren, and E. E. Tornau, Physica C **242**, 183 (1995).

[12] S. Lapinskas, E. E. Tornau, and A. Rosengren, Phys. Rev. B **52**, 15 565 (1995).

[13] P. E. Sterne and L. T. Wille, Physica C **162-164**, 223 (1989).

[14] E. Salomons and D. de Fontaine, Phys. Rev. B **41**, 11 159 (1990).

[15] E. E. Tornau, P. J. Kundrotas, S. Lapinskas, and A. Rosengren, Solid State Commun. **91**, 393 (1994).